MAK HILL Publications
Research Journal of Medical Sciences

Research Article
doi: 10.59218/makrjms.2024.1.1.10

Role of Magnetic Resonance Imaging in Evaluation of Intracerebral Ring Enhancing lesions and Correlation with MR Spectroscopy

[1]Pragya Ghosh, [2]Sunny Gupta and [3]Arnab Chaudhuri
[1-3]*Department of Radiodiagnosis, Heritage Institute of Medical Sciences, Bhadwar, Varanasi (U.P.) India*

OPEN ACCESS

Key Words
MRI, MRS, neurocysticercosis (NCC), tuberculoma, metabolites, ring lesion

Corresponding Author
Pragya Ghosh,
Department of radiodiagnosis, heritage institute of medical sciences, bhadwar, varanasi (U.P.) India

Author Designation
[1]Associate Professor
[2-3]Junior Resident

Received: 10 October 2023
Accepted: 25 October 2023
Published: 26 October 2023

Citation: Pragya Ghosh, Sunny Gupta and Arnab Chaudhuri, 2023. Role of magnetic resonance imaging in evaluation of intracerebral ring enhancing lesions and correlation with MR Spectroscopy. Res. J. Med. Sci., 18: 1-10, doi: 10.59218/makrjms.2024.1.1.10

ABSTRACT
Intra cerebral ring enhancing lesions are frequently encountered lesions with various etiologies. Conventional Magnetic Resonance Imaging (MRI) together with Magnetic Resonance Spectroscopy (MRS) narrows the differential diagnosis, thus aiding in better clinical management. To evaluate the role of conventional MRI together with MRS in assessing and differentiating various intra cerebral ring enhancing lesions. Present study is a retrospective, observational, cross sectional study of 100 patients diagnosed with cerebral ring enhancing lesions on contrast MRI study with MRS as an adjunct. Conventional MRI features on various sequences like T1W, T2W, Fluid attenuated inversion recovery (FLAIR), Diffusion weighted imaging (DWI) and post contrast (Injection Gadolinium) were recorded together with MRS spectra of various metabolite peaks like N-Acetyl Aspartate (NAA), Choline (Cho), Creatine (Cr), amino acids, lipid, lactate peaks with special emphasis on Cho/Cr ratio to differentiate various pathologies. The most prevalent etiology amongst the 100 patients studied was NCC (28%), closely followed by tuberculoma(27%), and Glioblastoma multiformae(09%). Majority of NCC lesions were T2W hyperintense and tuberculoma were T2W hypointense with prominent aminoacid peaks in NCC, lipid lactate peaks in tuberculoma. Cho/Cr ratio was <1 in majority of NCC and >1 in most of tuberculoma cases. Glioblastoma multiformae (GBM) patients showed Cho/Cr ratio <2 with shaggy ring enhancement, Primary CNS Lymphoma patients having Cho/Cr ratio >2 with cases of Pyogenic abscess showing smooth rim enhancement and central diffusion restriction. Cysts with mural nodule tumours (CMNT) including Hemangioblstoma and Pilocytic Astrocytoma were primarily located in cerebellum showing avid ring enhancement of nodule with demyelinating tumours showing open ring enhancement Intracerebral ring enhancing lesions were accurately diagnosed by conventional MRI together with MRS thus paving the way for a better clinical management of the patient.

INTRODUCTION

Intracerebral ring enhancing lesions are a commonly encountered diagnostic dilemma in neuroimaging[1]. Various imaging techniques like computed tomography and MRI are widely used for the diagnosis. These ring lesions are described as areas of hypointensity surrounded by a peripheral rim of enhancement after Gadolinium (Gad.) injection on MRI[2].

Ring enhancing lesions maybe single or multiple, maybe located in left or right side of brain or bilateral with varying amount of perifocal edema. Commonly they are noted at gray-white junction but can be subcortical, cortical or in deep white matter[1].

The various etiologies of ring lesions include infective causes (mainly NCC, tuberculoma, Pyogenic abscess), neoplastic (including GBM, metastasis, Primary CNS lymphoma, CMNT tumours (Hemangioblastoma and Pilocytic astrocytoma), Demyelinating disorders (multiple sclerosis, tumefactive demyelination) and vascular (Arteriovenous malformation, early subacute infarct) etc.

Conventional MRI is unable to differentiate between various infective etiologies or between neoplastic and non-neoplastic etiologies. Newer imaging techniques like proton MRS, DWI, perfusion weighted imaging are utilized to increase the specificity of diagnosis[3]. MRS is now being commonly used as an adjunct with routine MRI due to its increased specificity of differentiating various lesions. MRS measures the concentration of different metabolites in cerebral tissue like NAA, Choline, Creatine, lactate, lipids, various amino acids like glutamate (Glx), acetate and succinate. Various diseases show different concentration of these metabolites in cerebral tissue which aids in narrowing the differentials and helping in better management of the patient.

MATERIALS AND METHODS

Ethical approval: Our research began after approval from the Institutional ethical committee. Steps followed were in accordance with ethical standards of the institutional committee.

Study design: Retrospective / Cross Sectional

Study type: Observational

Setting: Hospital based setting in the department of Radiodiagnosis, Heritage Institute Of Medical Sciences, Varanasi

Age group and gender: All age groups and both genders with confirmed intracranial ring lesions

Inclusion criteria: Patients diagnosed with intracerebral ring enhancing lesions on contrast MRI brain.

Exclusion criteria: Patients without confirmed intracerebral ring lesions on MRI brain.

Sample size: 100 patients referred to Department of radiodiagnosis for MRI scan, Heritage Institute of Medical Sciences between the period of 1st-30th June-July 2022-2023.

Patient consent: Not applicable.

Investigation: MRI scan was done on MRI Philips achieva d Stream 3.0 tesla machine with proton spectroscopic capability using standard head coils and quantum gradients. Conventional MRI sequences including T1W, T2W, FLAIR, DWI sequences were taken. Post contrast images were taken using injection meglumine gadoterate (0.2 mL kg^{-1} body weight). MR spectroscopy was performed using single and multiple voxels technique with voxel placed around the region of interest.

Statistical analysis: For statistical analysis, data was entered into a Microsoft excel spreadsheet and then analyzed by SPSS (version 27.0; SPSS Inc., Chicago, IL, USA) and GraphPad Prism version[5]. Data had been summarized as mean and standard deviation for numerical variables and count and percentages for categorical variables. Two-sample t-tests for a difference in mean involved independent samples or unpaired samples. Paired t-tests were a form of blocking and had greater power than unpaired tests. A chi-squared test (χ^2 test) is any statistical hypothesis test where in the sampling distribution of the test statistic is a chi-squared distribution when the null hypothesis is true. Without other qualification, ‘chi-squared test’ often is used as short for Pearson’s chi-squared test. Unpaired proportions were compared by Chi-square test or Fischer’s exact test, as appropriate.

Explicit expressions that can be used to carry out various t-tests are given below. In each case, the formula for a test statistic that either exactly follows or closely approximates a t-distribution under the null hypothesis is given. Also the appropriate degrees of freedom are given in each case. Each of these statistics can be used to carry out either a one-tailed test or a two-tailed test.

Once a t-value is determined a p-value can be found using a table of values from Student’s t-distribution .If the calculated p-value is below the threshold chosen for statistical significance (usually the 0.10 the 0.05 or 0.01 level), then the null hypothesis is rejected in favour of the alternative hypothesis. p-value$\leq$0.05 was considered for statistically significant.

RESULTS

In our study a total of 100 patients were included. In our study, 29(29.3%) patients were ≤20 years of age, 17 (17.2%) patients were 21-30 years of age, 13(13.1%) patients were 31-40 years of age, 16(16.2%) patients were 41-50 years of age, 10(10.2%) patients were 51-60 years of age and 14(14.1%) patients were ≥61 years of age (Table 1). The above table also shows that the mean Age Mean±SD of patients was 35.4040±18.8468. In our study, 45 (45.5%) patients were Female and 54 (54.5%) patients were male (Table 2). In this study, majority of patients presented with seizures (75%), followed by headache (40%), vomiting (25%), fever (18%) and limb weakness (15%). In our study, 28 (28.0%) patients had Neurocysticercosis, 27(27.0%) patients had tuberculoma, 9 (9.0%) patients had Glioblastoma multiforme, 5 (5.0%) patients had Primary CNS lymphoma, 6 (6.0%) patients had Pyogenic abscess and 5 (5.0%) patients had Early subacute infarct (Table 3, Fig. 1).

T1W hypointensity was noted in 15 patients of NCC (54%), 12 patients of tuberculoma (44%), 08 cases Flair suppression noted in 14 patients of NCC (50%) and 02 cases of tuberculoma (7%), Rest of the flair of GBM 05 patients(100%) of Primary CNS lymphoma, both cases of fungal granulomas and multiple sclerosis 100% cases of pyogenic abscess (06) and early subacute infarct (05), 02 cases (62%) of metastasis (Table 4, Fig. 2-10).

Whereas T1W isointensity noted in 12 cases of NCC (42%), 15 cases of tuberculoma (55%), 01 case of GBM, mural nodule of all cases of Hemangioblastoma, Pilocytic astrocytoma and PXA (Table 4, Fig. 3-8).

Table 1: Distribution of age in group

Age in group	Frequency	Percentage
≤20	29	29.3
21-30	17	17.2
31-40	13	13.1
41-50	16	16.2
51-60	10	10.1
≥61	14	14.1
Total	99	100.0

Table 2: Distribution of sex

Sex	Frequency	Percentage
Female	45	45.5
Male	54	54.5
Total	99	100.0

Table 4: Distribution of findings on MRI sequences

Lesions	No.	T1W	T2W	FLAIR	DW1	Post Gad Enhancement
NCC	28	Hypointense in 15 Isointense in 12	27-Hyperintense with a hypointense rim, eccentric scolex in 10	FLAIR suppresion in 14 patients	Mild peripheral diffusion restriction in 02	Smooth rim enhancement in 26 cases
Tuberculoma	27	15- isointense , 12- hypointense	Hypointense core with an iso to hyperintense rim in 25 patients	FLAIR suppression in 02	Diffusion restriction in 05	Slightly irregular thicker ring enhancement in 26 cases
GBM	09	Hypointense in 08, isointense in 1	Hyperintense in all with central heterogenous Signal s/o necrosis and hemorrhage in all	Hyperintense in 08 Isointense in 01	Peripheral diffusion restriction in solid component in all	Thick irregular ring enhancement with shaggy inner margins in all
Primary CNS Lymphoma	05	Hypointense in all	Isointense in 04, hyperintense 01	Isointense in 04, hyperintense in 01	Patchy diffusion restriction in all	Moderate to intense contrast enhancement in all
Hemangioblastoma	03	Large cystic component with an eccentric solid mural nodule. Nodule isointense to grey matter in all , cystic component hypointense in all	Heterogenous hyperintense mural nodule in all Hyperintense cystic component in all	Hyperintense solid nodule and cystic component in all	Diffusion restriction in nodule in all	Avid ring enhancement of nodule in all
Pilocytic Astrocytoma	02	Both cases showed a cyst with a mural nodule, hypointense 01, isointense 01, cystic component hypointense in both	Nodule and cystic component hyperintense in both cases	Nodule and cystic part hyperintense in both cases	No diffusion restriction in both	Intense ring enhancement
Pleomorpic Xantho Astrocytoma	01	Cyst with a mural nodule, solid nodule iso intense to gery matter cystic component hypointense	Nodule and cystic component hyperintense to grey matter	Nodule and cystic component hyperintense to	No diffusion restriction	Moderate ring enhancement
Pyogenic Abscess	06	Hypointense core in all with mildly hypointense	Hyperintense core with hypointense rim in all	Hyperintense core with hypointense rim in all	Central diffusion restriction in all cases	Smooth moderate ring enhancement with thicker rim at rim in 03 cortical aspect in all
Metastasis	03	Hypointense in 02, isointense 01	Hyperintense in all	Hyperintense in all	No diffusion restriction with edema showing facilitated diffusion	Thick rim enhancement in all
Meningioma01		Solid with cystic component, dural based mass Solid Component isointense part to gery	Solid component isointense, cystic component hyperintense	Solid component isointense, cystic hyperintense	Mild peripheral diffusion restriction in solid component	Thick irregular ring enhancement in solid matter hypointense component
Tumefactive Demyelination	02	Hypointense in both	Hyperintense in both	Hyperintense in both	Mild peripheral diffusion restriction	Open ring enhancement in both, thinner at cortical side
Fungal Granuloma	02	Hypointense in both	Hyperintense core with hypointense rim in both	Hyperintense core with hypointense rim in both	No diffusion restriction	Thick rim enhancement with a nodular component in both
Multiple Sclerosis	02	Hypointense in both	Hyperintense in both with presence of Dawson's fingers.	Hyperintense	Mild peripheral diffusion restriction	Open ring enhancement in both thiner at cortical aspect
Toxoplasmosis	01	Hypointense	Hypointense	Hypointense	No diffusion restriction	Ring enhancement with a nodular component
Early Subacute Infarct	05	Hyperintense in all	Hyperintense in all	Hyperintense in all	Diffusion restriction in all	Thin ring enhancement in all
Early Subacute Hemorrhagic Contusion	03	Isointense in 02, hypointense in 01	Hypointense in 02 , hyperintense in 01	Hypointense in 02, hyperintense in 01	No diffusion restriction	Thin ring enhancement in all

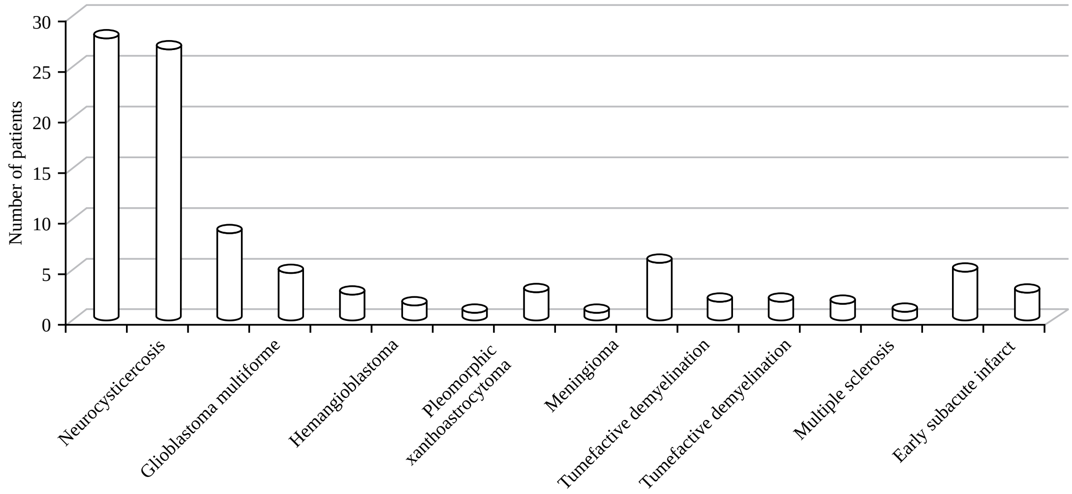

Fig. 1: Bumber of patients

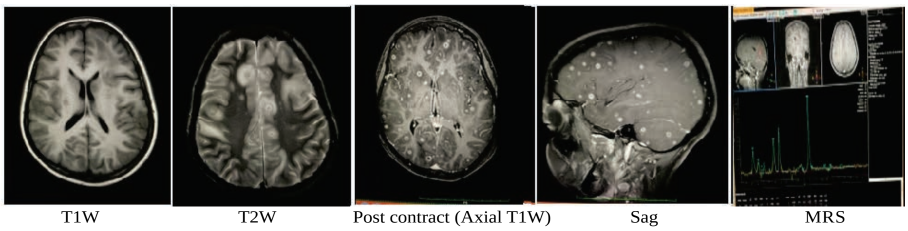

Fig. 2: NCC

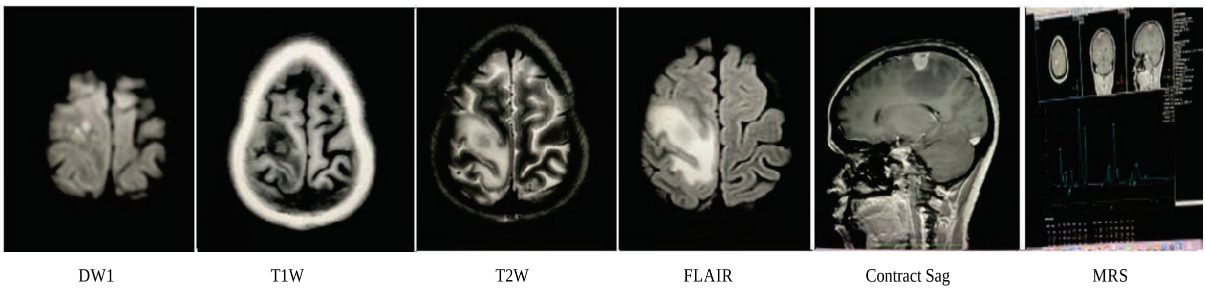

Fig. 3: Tuberculoma

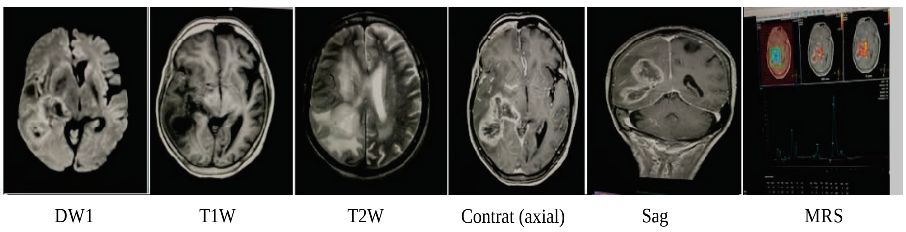

Fig. 4: GBM

/FLAIR hyperintensity noted in 27 patients of NCC(96%), 100% cases of GBM, Hemangioblastoma, Pilocytic astrocytoma, PXA, Pyogenic abscess, metastasis and early sub acute infarct whereas 25 cases of tuberculoma (93%) showed a T2W hypointense core with a hyperintense rim (Table 4). sequences follow findings of T2W sequences (Table 4).

Diffusion restriction noted in 02 cases of NCC (07%), 05 cases of tuberculoma (18%), 100% cases of

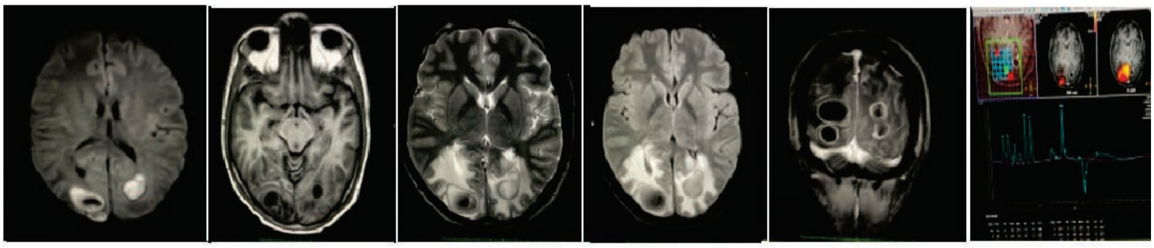

Fig. 5: Pyogenic abscess

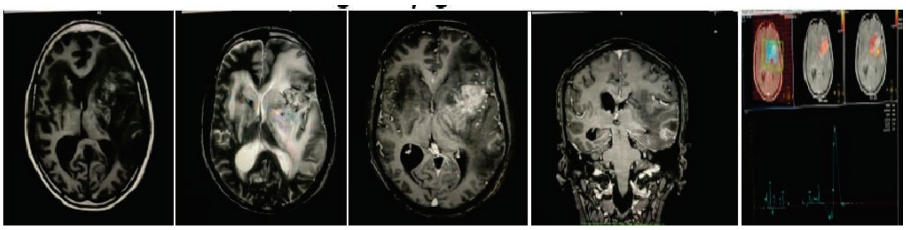

Fig. 6: Fungal granuloma

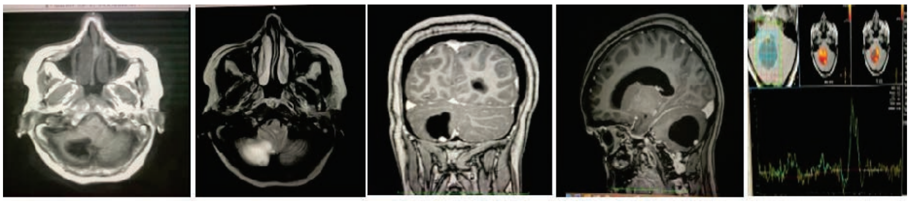

Fig. 7: Hemangioblastoma

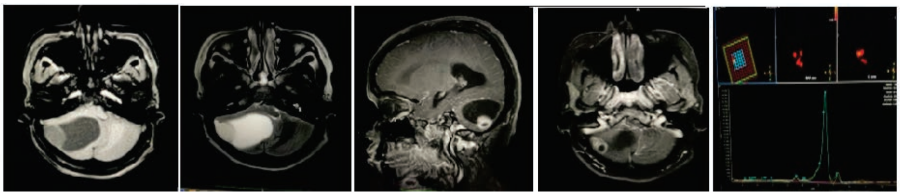

Fig. 8: Pilocytic astrocytoma

Table 5: Distribution of commenest location (Lobes)

Case	Commenest location (Lobes)	Frequency	Total
Neurocysticercosis	Fronto - parietal	10	28
Tuberculoma	parietal	07	27
Glioblastoma multiforme	Occipito - parietal	03	9
Primary CNS lymphoma	Fronto -temporo - parietal	03	5
Hemangioblastoma	cerebellum	03	3
Pilocytic astrocytoma	cerebellum	02	2
Pleomorphic xanthoastrocytoma	right high frontal	01	1
Metastasis	Fronto - temporo- parietal	03	3
Meningioma	High fronto parietal lobe	0	1
Tumefactive demyelination	Fronto- parietal	01	2
Pyogenic abscess	Occipital	04	6
Fungal granuloma	fronto - temporo - parietal	02	2
Multiple sclerosis	Fronto - parietal	02	2
Toxoplasmosis	Fronto - temporo- parietal	01	1
Early subacute infarct	Temporal	03	5
Early subacute hemorrhagic contusion	Frontal	02	3

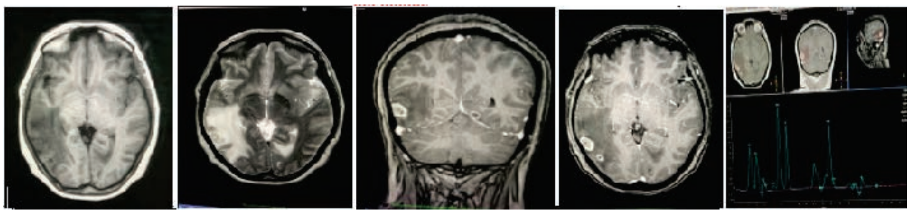

T1W T2W Post Gad (cor) Axail MRS

Fig. 9: Metastasis

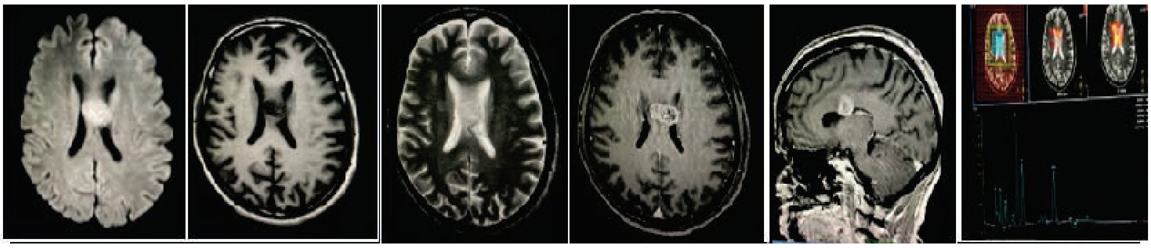

DW1 T1W T2W Post Gad (axail) Sag MRS

Fig. 10: Primary CNS lymphoma

Table 6: Distrubution of choline/cr ratio and other significant mrs findings

Lesions	Choline / cr ratio	Total cases	Other MRS findings
Neurocysticercosis	<1 = 20	28	Prominent acetate peak In 26, succinate peak in 25.
Tuberculoma	>1 = 24	27	Prominent lipid lactate peaks in all, reduced NAA/Cr in 24.
Glioblastoma multiforme	<2 = 06 , >2 = 03	09	Reduced NAA In 09 , prominent lipid lactate peaks In 09
Primary CNS lymphoma	>2 = 04	05	Prominent lipid lactate peaks in 05, reduced NAA in 05 , small amino acid peaks in all
Hemangioblastoma	<2 = 03	03	Reduced NAA in all ,small lipid peaks and amino acid peaks in all
Pilocytic astrocytoma	>3 = 02	02	Reduced NAA In 02, lipid and amino acid peaks in 02, reduced NAA/ Cho, reduced NAA/Cr In 02
Pleomorphic xanthoastrocytoma	<2=01	01	Reduced NAA , prominent lipid, amino acid peaks
Metastasis	<3 = 02 , >3 = 01	03	Reduced NAA/Cr in 03, prominent lipid lactate peaks in 03, prominent Glx peak in 03
Meningioma	>2	01	Prominent amino acid peaks esp. alanine , small lipid peak, Reduced NAA
Pyogenic abscess	<2 = 04 , >2 = 02	06	Prominent lipid lactate peaks in 06, amino acid peaks in 06
Tumefactive demyelination	<2 = 02	02	Reduced NAA In 02 , reduced NAA / Cho, increased Cho / NAA in 02 , small lipid lactate peaks, Glx in 02
Fungal granuloma	<2 = 02	02	Lipid lactate peaks, amino acids peak In 02 , reduced NAA/Cr In 02
Multiple sclerosis	<2 = 02	02	Reduced NAA / Cr in 02 , slightly decreased NAA , increased Cr in 02
Toxoplasmosis	<2	01	Prominent lipid lactate peak in 01, reduction Of NAA, reduced Choline and Creatine
Early subacute infarct	>1 = 03 , <1 = 02	05	Prominent lactate peak In 03, mild reduction Of NAA in 04 , normal Choline in 05
Early subacute hemorrhagic contusion	<2 = 03	03	Reduced NAA In 03, increased Choline In 03, small lactate peaks, Glx peak in 03

GBM, Primary CNS lymphoma, Pyogenic abscess, Hemangioblastoma and early subacute infarct (Table 4, Fig. 2, 4, 5, 10).

Post gadolinium study showed smooth rim enhancement in 26 cases of NCC(93%), slightly thicker ring enhancement in 26 cases of tuberculoma (93%), thick irregular ring enhancement with shaggy margins in 100% cases of GBM, avid ring enhancement in all cases of CMNT tumors, smooth moderate ring enhancement with thicker rim at cortical aspect in 06 (100%) cases of pyogenic abscess, thick rim enhancement in 100% cases of metastasis with open ring enhancement (thinner at cortical aspect) in 100% cases of tumefactive demyelination and multiple sclerosis (02 each) (Table 4, Fig. 2-10).

In our study the commonest location of NCC was fronto-parietal lobe (36%), parietal lobe in Tuberculoma (26%), Occipito–parietal lobe in GBM (33%), Cerebellum in Hemangioblastoma and Pilocystic Astrocytoma (100%), occipital lobe in Pyogenic abscess (67%), Fronto-temporo-parietal lobe in Primary CNS Lymphoma (60%) and temporal lobe in early sub acute infarct (60%).

In our study, 71% patients of NCC had Cho/Cr ratio <1 with prominent acetate and succinate peaks in 93% and 89% patients respectively. 89% of tuberculoma patients had Cho/Cr >1 with prominent lipid lactate peaks in all. 33% patients of GBM had Cho/Cr >2 with 67% having Cho/Cr ratio<2 with prominent lipid lactate peaks, raised Cho/NAA, reduced NAA/Cr in all. 80% cases of Primary CNS Lymphoma had Cho/Cr >2 with prominent lipid lactate peak and reduced NAA in all. 100% patients of Hemangioblastoma and PXA had Cho/Cr <2 with Cho/Cr >3 in all patients of Pilocytic Astrocytoma with reduced NAA, prominent lipid and amino acid peaks in all. 67% patients of metastasis had

Table 7: Association between all cases vs site site

Case	Left	Right	Bilateral	Total
Neurocysticercosis	9	7	12	28
Tuberculoma	10	14	3	27
Glioblastoma multiforme	3	6	0	9
Primary CNS lymphoma	3	1	1	5
Hemangioblastoma	1	2	0	3
Pilocytic astrocytoma	1	1	0	2
Pleomorphic xanthoastrocytoma	0	1	0	1
Metastasis	0	0	3	3
Meningioma	0	1	0	1
Tumefactive demyelination	1	1	0	2
Pyogenic abscess	3	1	2	6
Fungal granuloma	0	0	2	2
Multiple sclerosis	0	0	2	2
Toxoplasmosis	0	0	0	1
Early subacute infarct	3	2	0	5
Early subacute hemorrhagic contusion	1	0	2	3

Table 8: Association between all cases vs size of lesions (cm) size of rings (cm)

Case	<1 c m	1-2 cm	2-4 cm	>4 cm
Neurocysticercosis	23	5	0	0
Tuberculoma	13	14	0	0
Glioblastoma multiforme	0	2	7	0
Primary CNS lymphoma	0	0	1	4
Hemangioblastoma	0	0	0	3
Pilocytic astrocytoma	0	0	1	1
Pleomorphic xanthoastrocytoma	0	0	1	0
Metastasis	2	7	3	0
Meningioma	0	0	1	0
Tumefactive demyelination	0	1	1	0
Pyogenic abscess	0	6	5	2
Fungal granuloma	1	3	4	1
Multiple sclerosis	0	2	0	0
Toxoplasmosis	0	3	1	1
Early subacute infarct	0	2	3	0
Early subacute hemorrhagic contusion	0	2	1	0

Cho/Cr <3, 33% having Cho/Cr >3 with prominent lipid lactate and Glx peaks, reduced NAA/Cr in all. 67% patients of Pyogenic abscess, 100% patients of tumefactive demyelination, fungal granuloma, multiple sclerosis, toxoplasmosis, early subacute hemorrhagic contusion had Cho/Cr <2.

Prominent lipid lactate peaks noted in all cases of metastasis, fungal granuloma multiple sclerosis with prominent lactate peak in 60% cases of early subacute infarct. Reduced NAA/Cr noted in all cases of metastasis, multiple sclerosis and fungal granuloma Meningioma patient had Cho/Cr >2with prominent amino acids peak especially alanine (Table 6).

16 patients of NCC, 19 patients of tuberculoma, 07 patients of GBM, 04 patients of Primary CNS lymphoma and 05 patients of Early subacute infarct had single rings. 12 patients of NCC, 04 patients of tuberculoma, 02 patients of GBM, 05 patients of Pyogenic abscess and 03 patients of early subacute hemorrhagic contusion had multiple rings.c 09 patients of NCC 10 patients of tuberculoma, 03 patients of GBM, 03 patients of Primary CNS lymphoma, 03 patients of Pyogenic abscess, and 03 patients of early subacute infarct showed ring lesions on left side. 07 patients of NCC, 14 patients of tuberculoma, 06 patients of GBM, and 02 patients of early subacute infarct had ring lesions on right side. 12 patients of NCC, 03 patients of tuberculoma, 03 patients of metastasis, and 02 patients of pyogenic abscess, fungal granuloma, early subacute hemorrhagic contusion had bilateral rings (Table 7).

23 patients of NCC, 13 patients of tuberculoma and 02 patients of metastasis had lesions <1cm. 05 patients of NCC, 14 patients of tuberculoma, majority of rings in metastasis(70%) and Pyogenic abscess(46%) were between 1-2cm in size. 07 cases of GBM(77%) had lesions of size between 2-4cm and 04 Primary CNS lymphoma and 03 patients of Hemangioblastoma patients had lesions >4 cm (Table 8).

20 patients of NCC, 20 patients of tuberculoma, 04 patients of Primary CNS lymphoma, 04 patients of early subacute infarct, 03 patients of early subacute hemorrhagic contusion had mild edema.

04 patients of NCC, 06 patients of tuberculoma, 03 patients of GBM and 05 patients of Pyogenic abscess had moderate edema. 05 patients of GBM and 01 patient of pyogenic abscess had severe edema.

DISCUSSION

Intra cerebral ring enhancing lesions pose a diagnostic dilemma in neuroimaging with various etiologies with overlapping findings on conventional MRI sequences. Newer imaging modalities like MRS help to narrow the differential diagnosis.

In our study, most of the patients were <20 years old (29.3%) which was statistically significant (p = 0.00068), (z = 3.395).

In our study the mean age of patients was (35.4040±18.8468) years. Similar findings were reported by Rajasree *et al.*[3] who recorded the mean age of patients 36.76+21.62 years whereas Joy *et al.*[4] reported in their study the mean age of patients 42.85+14.76 years.

Shetty *et al.*[5] found that the most common radiological abnormality seen in young Indian patients with epilepsy is a single small enhancing (ring/disc) computed tomographic lesion. They reported a case of 6 year old female who presented with complex partial seizures.

We found that male 54 (54.5%) population was higher than the female population 45 (45.5%) which was statistically significant (p = 0.20054), (z = 1.2792). Majority of patients presented with seizures(74%), followed by headache(40%) , vomiting(25%), fever (18%) and limb weakness(15%) corresponding to findings of Elsadway *et al.*[2].

Khatri *et al*[6] examined that the causative organism, Mycobacterium tuberculosis, incites a granulomatous inflammatory response in the brain, the effects of which can be appreciated on MRI which can thus be used for diagnosis of the same. They evaluated 40 patients and found 18 cases of tuberculoma, 10 of NCC, 04 abscesses, 04 metastases, 02 cases of primary brain tumors and 02 cases of toxoplasmosis. The highest incidence of ring lesions were found in 21-30 years age group.

In our comprehensive analysis of 100 patients presenting with ring enhancing lesions we categorized them into distinct diagnostic groups based on their neuroimaging findings. NCC(28.0%) and Tuberculoma (27.0%) were the most prevalent etiologies corresponding to the study by Mirchandani *et al.*[7]., Bava *et al.*[8] followed by GBM(9.0%), Primary CNS lymphoma(5.0%), Pyogenic abscess(6.0%) and early subacute infarct (5.0%).

The high prevalence of NCC and tuberculoma underscores the significance of infectious etiologies in our patient population which is consistent with the endemic nature of these diseases in our region. These findings emphasize the importance of early detection and timely management to prevent potentially severe neurological complications.

GBM and Primary CNS Lymphoma, although less frequent, demand special attention due to their malignant nature. Accurate diagnosis and prompt intervention are crucial to improve patient outcomes in these cases.

Pyogenic abscesses represent another significant portion of our cohort, necessitating aggressive antimicrobial therapy and surgical intervention. Identifying the causative pathogens and tailoring treatment strategies are paramount this was statistically significant ($p<.00001$), ($z = 5.4269$).

This study provides valuable insights into the radiological characteristics of various intracranial pathologies, aiding in their differentiation and clinical management. Notably, the T1-weighted (T1W) hypo to isointensity was a common feature in NCC and tuberculoma cases, suggesting their potential overlap in imaging appearance but T2W hyperintensity favours NCC and T2W hypointensity favours caseating tuberculomas, reflecting the inflammatory and edematous nature of these conditions. T2W hypointense NCC poses a diagnostic challenge and their incomes the role of MRS which helps us to correctly identify the lesion. MRS demonstrates the various metabolites and their ratios like Choline, Creatine, NAA ,various aminoacids (like acetate, succinate ,alanine),lipid, lactate which helps to narrow the differentials of ring lesions.

In our study one case of NCC was T2W hypointense whereas rest of the cases showed T2W hyperintensity. Also NCC demonstrated a Cho/Cr ratio<1 in 71% of cases, accompanied by prominent acetate and succinate peaks in 93% and 89% case respectively. Tuberculoma cases exhibited a Cho/Cr ratio >1 in 89% of cases along with prominent lipid lactate peaks in all cases. Similar results were reported by Rajasree *et al.*[3] and Gupta *et al.*[9]. Lipid peak in tuberculoma is mainly due to high lipid content in the cell walls of tubercular bacillus and lactate represents the necrosis and anaerobic glycolysis within tuberculoma.

Primary CNS lymphoma, Pyogenic abscess, showed T1W hypointensity in all cases with GBM being T1W hypointense in 89% cases emphasizing the importance of recognizing these unique signatures. T2W and FLAIR hyperintensity findings were a hallmark of NCC (96%), GBM, Hemangioblastoma, Pilocytic Astrocytoma, PXA, metastasis and early subacute infarct(100%) with all cases of Pyogenic Abscess demonstrating a hyperintense core with a hypointense rim serving as a potential diagnostic clue.

Diffusion restriction was a consistent feature in GBM, Primary CNS lymphoma, Pyogenic abscess and early subacute infarcts, underscoring its utility in distinguishing these entities. Post-gadolinium imaging further enhanced diagnostic precision with the specific patterns of rim enhancement. For instance the smooth ring enhancement in NCC, thicker ring in tuberculoma was indicative of a more benign nature while the shaggy margins in GBM denoted its aggressive behaviour with the hyperintense rim around necrotic core due to deposition of hemorrhagic products.

Also central diffusion restriction noted in core of pyogenic abscess against peripheral diffusion restriction in GBM, corresponding to a study by Toh *et al*.[10] Contrastingly, CMNT tumours displayed avid ring enhancement, emphasizing the need for careful evaluation to rule out malignancy.

Post gadolinium study showed smooth ring enhancement with thicker rim at cortical aspect in all cases of pyogenic abscess with open ring enhancement (thinner at cortical aspect) in all cases of tumefactive demyelination and multiple sclerosis. Similar findings were reported by Garg *et al.*[1] in their study.

In a study by Ram *et al.*of 50 cases, majority of lesions were tuberculoma followed by metastasis and NCC with majority of lesions being multiple (62%) and (60%) smaller in size (< 2cm). Overall sensitivity and accuracy of MR were 81.54%, 92.76% and MRI+MRS were 91.27% and 96.80% respectively.

Our study provides valuable insights into the common locations of various intracranial pathologies, aiding in their clinical recognition and localization. Notably, the fronto-parietal lobe emerged as the most common site for NCC, highlighting its predilection for this cerebral region. Similarly, tuberculoma was frequently found in the parietal lobe, while GBM showed a distinct preference for the occipito-parietal lobe, indicative of its aggressive and infiltrative nature. In contrast, hemangioblastoma and pilocytic astrocytoma exhibited a striking affinity for the cerebellum which is in line with their characteristic appearances in posterior fossa location. Pyogenic abscesses were commonly located in the occipital lobe, emphasizing the importance of considering infectious etiologies in cases presenting with posterior cerebral involvement.

Primary CNS lymphoma a malignant entity, predominantly affected the fronto-temporo-parietal lobes, reflecting its propensity to involve multiple brain regions. Early subacute infarcts were notably situated in the temporal lobe which aligns with the vascular supply patterns in this region. NCC demonstrated a Cho/Cr ratio <1 in 71% of cases, accompanied by prominent amino acid peaks. Tuberculoma cases exhibited a Cho/Cr ratio >1 in 89% of patients, along with prominent lipid lactate peaks in all cases. Several studies have documented increased choline levels with higher grade tumours as aggressive tumours show increased membrane turnover and cellular density, However few higher grade tumours like GBM can have lower levels of choline with Cho/Cr ratio <2 due to necrotic cores In our study also majority of GBM (67%) had Cho/Cr ratio<2 with 33% having ratio>2 corresponding to a study by Howe *et al.*[11].

Reduced NAA and prominent lipid lactate peak was a dominant feature of GBM in our study which signifies the necrotic core of GBM. We had a single case of ring enhancing meningioma which showed Cho/Cr >2. with prominent alanine peak. Primary CNS lymphoma predominantly presented with a Cho/Cr ratio >2, prominent lipid lactate peaks and reduced NAA in 80% of cases.

Hemangioblastoma and PXA patients had a Cho/Cr ratio<2, but Cho/Cr>3 was observed in all Pilocytic Astrocytoma cases, along with reduced NAA and prominent lipid and amino acid peak. These findings were also reported by Manias *et al*.[12].

Metastasis cases had a varied Cho/Cr ratio, with 67% <3 and 33% >3, accompanied by prominent lipid lactate and Glx peaks, Pyogenic abscess, tumefactive demyelination, fungal granuloma, multiple sclerosis, toxoplasmosis and early subacute hemorrhagic contusion consistently had a Cho/Cr ratio <2.

In our study 57% patients of NCC, 70% patients of tuberculoma, 78% GBM patients had single rings with 43% cases of NCC, 14% of tuberculoma, 100% of metastasis, 84% of Pyogenic abscess patients and all cases of fungal granuloma and early subacute hemorrhagic contusion having multiple rings .

32% patients of NCC in this study, 37% of tuberculoma, 33% of GBM and 60% cases of primary CNS lymphoma had rings in the left cerebral hemisphere with 52% cases of tuberculoma, 25% of NCC, 67% of GBM patients having rings on right side with bilateral rings found notably in NCC (43%), metastasis(100%) and Pyogenic Abscess(33%).

In our study, 82% of NCC patients and 67% patients with tuberculoma had lesions <1 cm in size with 33% patients of tuberculoma, majority of patients with pyogenic abscess and metastasis had lesions of sizes between 1-2 cm.77% cases of GBM had lesions of size between 2-4 cm and majority of Primary CNS lymphoma and hemangioblastoma patients showed lesions >4 cm in size. 72% patients with NCC, 74% patients of tuberculoma had mild surrounding edema in our study with 22% cases of NCC and tuberculoma, 83% cases of pyogenic abscess showed moderate edema with severe edema noted in 55% cases of GBM and 16% cases of Pyogenic abscess.

Conventional Cerebral MRI imaging has a high sensitivity but relatively low specificity to delineate the different causes of ring enhancing lesions, to differentiate between infectious and neoplastic etiologies Kapsalaki *et al.*[13] with increased sensitivity (87.5%) and specificity (93.3%) with the incorporation of MRS Jesrani *et al.*[14].

In our study, MRS proved to be a helpful tool in differentiating between NCC and tuberculoma, between neoplastic and non neoplastic lesions (like GBM and Pyogenic abscess)as they share many common features on routine MRI. Currently researches are ongoing for evaluation of effectiveness of MRS and to add MRS with conventional MRI as a standard protocol for better diagnosis and management of the patients.

CONCLUSION

In conclusion this comprehensive study of 100 patients with intracranial lesions has provided significant insights into their demographics, radiological characteristics and distribution across different pathologies.

Patient demographics: The study revealed that the majority of patients were under the age of 20 with a statistically significant predominance. This finding suggests that intracranial lesions have a higher incidence in younger individuals in the studied population.

Gender distribution: While male patients slightly outnumbered female patients, the difference was not statistically significant. This observation highlights that intracranial lesions can affect both genders almost equally.

Prevalence of intracranial pathologies: NCC and tuberculoma were the most prevalent intracranial pathologies with a high prevalence of infectious etiologies. GBM and Primary CNS lymphoma, though less frequent, demand prompt and precise diagnosis due to their malignant nature. Pyogenic abscesses were also notable in the patient cohort, emphasizing the importance of tailored treatment strategies for these cases.

Radiological characteristics: The study delineated distinctive radiological features of different intracranial pathologies. These characteristics, including T1W hypointensity, T2W flair hyperintensity and diffusion restriction, serve as valuable diagnostic markers. Post-gadolinium imaging further enhanced diagnostic precision, especially in differentiating benign from malignant lesions.

Location of lesions: The anatomical localization of lesions varied among different pathologies, aiding in their clinical recognition. Understanding these patterns is vital for precise diagnosis and treatment planning.

Metabolic profiles: The spectroscopic analysis provided insights into the metabolic profiles of intracranial lesions, enabling differentiation based on Cho/Cr ratios and the presence of prominent peaks. This information can aid in the selection of appropriate diagnostic and therapeutic approaches.

REFERENCES

1. Garg, R. and M. Sinha, 2010. Multiple ring-enhancing lesions of the brain. J. Postgrad. Med., 56: 307-316.
2. Elsadway, M.E. and H.I. Ali, 2018. Verification of brain ring enhancing lesions by advanced mr techniques. Alexandria. J. Med., 54: 167-171.
3. Rajasree, D., T.L. Kumar and K. Vijayalakshmi, 2020. Role of magnetic resonance spectroscopy in the evaluation of ring enhancing lesions of the brain. J. Clin. Diagn. Res., 14: 10-14.
4. Joy, L. and A.K. Sakalecha, 2023. Role of multiparametric magnetic resonance imaging of the brain in differentiating neurocysticercosis from tuberculoma. Cureus., Vol. 14. 10.7759/cureus.39003
5. Shetty, G., K.S. Avabratha, B.S. Rai, 2014. Ring-enhancing lesions in the brain: A diagnostic dilemma. Iran. J. Child. Neurol., 8: 61-64.
6. Khatri, G.D., V. Krishnan, N. Antil and G. Saigal, 2018. Magnetic resonance imaging spectrum of intracranial tubercular lesions: One disease, many faces. Pol. J. Radiol., 83: 628-639.
7. Mirchandani, S., J. Dave and A.N. Dave, 2019. Role of MRI and MR spectroscopy (metabolic mapping) in characterisation of ring enhancing lesions in brain. J. Dent. Med. Sci., 18: 10-55.
8. Bava, J.S., A. Sankho, S. Patil, 2016. Role of MR spectroscopy in evaluation of various ring enhancing lesions in brain. Int. Sci. Res., 5: 2-14.
9. Gupta, R.K., K.M. Hasan, A.M. Mishra, D. Jha, M. Husain, K.N. Prasad and P.A. Narayana, 2005. High fractional anisotropy in brain abscesses versus other cystic intracranial lesions. AJNR. Am. J. Neuroradiol., 26: 1107-1114.
10. Toh, C.H., K., C. Wei, C., N. Chang, P. ,W Hsu and H. ,F Wong et al., 2012. Differentiation of pyogenic brain abscesses from necrotic glioblastomas with use of susceptibility-weighted imaging. Am. J. Neuroradiol., 33: 1534-1538.
11. Howe, F.A., S.J. Barton, S.A. Cudlip, M. Stubbs and D.E. Saunders et al., 2003. Metabolic profiles of human brain tumors using quantitative in vivo 1H magnetic resonance spectroscopy. Magn. Reson. Med., 49: 223-232.
12. Manias, K., S.K. Gill, N. Zarinabad, P. Davies and M. English et al., 2017. Evaluation of the added value of 1H-magnetic resonance spectroscopy for the diagnosis of pediatric brain lesions in clinical practice. Neuro. Oncol. Pract., 5: 18-27.
13. Kapsalaki, E., E.D. Gotsis, I. Tsougos, K.N. Fountas, 2012. The Role of Magnetic Resonance Spectroscopy in the Diagnosis of Ring Enhancing Lesions. Rijeka, Croatia,, ISBN-17: 978-953-51-0200-7, Pages: 158.
14. javed, K., H.A. Butt, H.M.A. Jamil, A.U. Kamran, B. Nadeem, F. Shahid and I. Uddin, 2022. Diagnostic accuracy of magnetic resonance spectroscopy in differentiating malignant and benign brain lesions. Pak. J. Med. Health. Sci., 16: 528-530.